Atmospheric Environment 290 (2022) 119275

Contents lists available at ScienceDirect

Atmospheric Environment

journal homepage: www.elsevier.com/locate/atmosenv

How trees affect urban air quality: It depends on the source

Tom Grylls, Maarten van Reeuwijk *

Imperial College London, Department of Civil and Environmental Engineering, SW7 2AZ, London, United Kingdom

HIGHLIGHTS

- Large-eddy simulations used to analyse the impacts of trees on urban air quality.
- Thermal effects (convection, shading and transpiration) are important to consider.
- Tree impact is driven by the balance between deposition and dispersion effects.
- Proximity to local pollution source alters the impact of a tree.
- Trees effects are amplified in conditions conducive of poor air quality.

ARTICLE INFO

Keywords:
Trees
Urban
Air pollution
Deposition
Shading
Transpiration
Large-eddy simulation

ABSTRACT

Large-eddy simulation (LES) is used to systematically analyse the impacts of trees on air quality in idealised street canyons. The LES tree model includes radiation, transpiration, drag and deposition effects. The superposition of background concentrations and local emissions is used to construct realistic urban scenarios for fine particulate matter (PM2.5) and nitrogen oxides (NO_x). Both neutral and convective atmospheric conditions are considered to assess the importance of buoyancy effects and the role of tree shading and transpiration. Tree impact on local air quality is shown to be driven by the balance between the rate at which they actively remove pollutants from the air (deposition) and the way in which they alter the transport of pollutants within and out of the street canyon (dispersion). For pollutant species or street types where the concentration field is dominated by background levels (such as PM2.5), deposition will generally dominate and thus local air quality will improve. For pollutants and street types where local emission sources dominate (e.g. NO_x on a busy road), the dispersion effects of trees become more prominent and can lead to elevated concentrations where mixing or exchange is significantly inhibited. Mixing in the convective simulation is more vigorous than in the neutral simulation which results in substantial differences in in-canyon flow fields and exchange velocities, highlighting the importance of incorporating thermal effects when studying urban trees. Increased residency times, and thus deposition, under neutral conditions suggest that trees can have amplified effects under conditions conducive of poor air quality. For the cases considered, trees largely act to improve air quality with the exception of localised hotspots. The competing effects of trees — specifically deposition versus altered exchange with the atmosphere — are also incorporated in a simple integral model that predicts whether or not the air quality will improve. The model matches well with LES predictions for both PM2.5 and NO_x and can serve as a simple tool for urban design purposes.

1. Introduction

Trees play an integral role in the climate of urban areas. They have been identified as potential solutions to two of the biggest challenges that cities face globally: urban air quality and the urban heat island effect (Akbari et al., 2001; Nowak and Heisler, 2010). The presence of trees within urban areas acts to alter the exchanges of momentum, radiation, temperature, humidity and pollution. These exchanges are highly complex and hence our understanding of and ability to quantify their direct effects remains limited (Grylls and van Reeuwijk, 2021).

Trees actively remove pollutants from the urban atmosphere via enhanced rates of deposition due to their relatively large surface area and, depending on the species, surface properties (Sæbø et al., 2012). However, they also impose drag on the surrounding urban flow field and

* Corresponding author.
E-mail address: m.vanreeuwijk@imperial.ac.uk (M. van Reeuwijk).

https://doi.org/10.1016/j.atmosenv.2022.119275
Received 1 May 2022; Received in revised form 3 July 2022; Accepted 5 July 2022
Available online 22 July 2022

subsequently can have adverse affects on pollutant dispersion (in particular in respect to the vertical exchange with the urban boundary layer aloft; Salim et al., 2015; Gromke et al., 2015). The role of trees in urban pollution dispersion is often characterised by this balance between their dispersive and depositional properties (Buccolieri et al., 2018). Janhäll (2015) reviewed these two dominant effects and concluded that there is a need for more integrated studies where they are both considered simultaneously. Recent studies have presented results where trees have both helped and hindered the local air quality (Jeanjean et al., 2017; Santiago et al., 2017). Abhijith et al. (2017) reviewed the existing field, experimental and numerical studies on trees and urban air pollution, and reported that on average, across all studies considered, trees had a detrimental effect (≈20–96% increase in local pollution concentrations). Buccolieri et al. (2018) reiterated this viewpoint in stating that whilst the problem is highly case-specific, in the majority of cases the reduced ventilation and increased drag induced by trees outweighs their active removal of pollutants from the urban atmosphere.

A key conclusion from all three review papers discussed above is that there is a need to also consider the thermal effects of trees (Janhäll, 2015; Abhijith et al., 2017; Buccolieri et al., 2018). Tree canopies alter the energy balance of the local microclimate (Grylls and van Reeuwijk, 2021). As a result, the distribution and magnitude of buoyancy sources and sinks within the urban canopy layer are different whether a tree is present or not. As well as the drag imposed by tree canopies, these thermal effects also significantly affect the dispersion of pollutants and therefore the local air quality.

In this paper, a recently developed tree model for large-eddy simulation (LES; Grylls and van Reeuwijk, 2021) is used that includes drag, shading, evaporation and deposition to determine the effect of trees on air quality. The tree model distinguishes between cooling via transpiration and shading. An attractive feature of the model is that it was designed to work with a minimal number of parameters. The model was previously used to provide insight into tree cooling regimes and LES was performed in the absence of urban morphology.

This paper uses the model to study the effect of trees in idealised street canyons. Radiative effects on pollutant transport are investigated by comparing simulations under neutral and convective atmospheric conditions, both with and without trees. We determine the effect of trees on air quality for two cases: one where the air pollution is caused solely by emissions inside the canyon, and another where it is the result of the background concentration level. These two scalar fields are then combined to create realistic scenarios in which 1) the pollution concentration is dominated by local emissions within the street canyon, as is often the case for nitrogen oxides (NO_x) on busy roads, and 2) the pollution concentration is dominated by background levels, as is typically the case for PM2.5 (Zhou and Lin, 2019; Fu et al., 2020).

The modelling and simulation details are outlined in Section 2. Results are presented in Section 3 for the flow and temperature fields and the effect of trees on local and background air pollution. The effect of trees on air quality is then investigated further through two scenarios – one associated with NO_x and one representtive of PM2.5 (Section 3.4). Section 4 outlines an integral model that provides insight into the key processes that determine whether trees are beneficial or detrimental for urban air quality. The results are discussed in 5, contextualising the findings against the complexity of real urban environments and analysing what it all means for urban design. Finally, conclusions are drawn in Section 6.

2. Large-eddy simulation set-up

Large-eddy simulation models provide the ability to simulate the urban microclimate at very high resolutions (O(1 m, 0.1 s)) and therefore to resolve the turbulent urban flow field and its interaction with tree canopies. The tree model of Grylls and van Reeuwijk (2021) provides the capability to study the integrated (dispersive, depositional and thermal) effects of trees and therefore, when coupled with an LES model, to study the role of trees in the urban climate. In this section, the modelling details and simulation set-up for the systematic investigation into the role of trees within an infinite street canyon is outlined.

2.1. uDALES

The urban large-eddy simulation model uDALES is used to simulate trees in the urban microclimate. uDALES is an atmospheric large-eddy simulation model that has been adapted to study the urban microclimate (Heus et al., 2010; Suter et al., 2020). uDALES is able to capture wet thermodynamics, idealised and realistic urban morphologies, urban surface energy balances, non-neutral boundary layers and real-time pollution dispersion (Suter, 2018; Grylls, 2019; Grylls et al., 2019, 2020, 2021; Sützl et al., 2021; Suter et al., 2021).

The immersed boundary method and logarithmic wall functions are used to model buildings within the domain (Tomas et al., 2016; Suter, 2018). uDALES uses a spatial discretisation on an Arakawa C-grid, a second-order central-differencing scheme for velocity u_i, temperature θ and humidity q_v, a κ-scheme for pollution concentrations and a Runge-Kutta time-integration scheme (Hundsdorfer et al., 1995; Heus et al., 2010).

2.2. Tree model

The tree model of Grylls and van Reeuwijk (2021) is used to capture the drag, shading, transpiration and deposition effects of tree canopies on the surrounding air. The model captures the effects of trees on the surrounding environment at the 'grey-scale'. Tree and environmental parameters are used to calculate volumetric source/sink terms, S, in real time that represent the effect of a section of tree canopy at the resolution of the LES model (O(1 m, 0.1 s)).

For example, the deposition of pollutants onto the tree canopies introduces the sink term S_φ into the governing equation for relevant low-pass-filtered pollutant concentration fields, φ,

$$\frac{\partial \varphi}{\partial t} = -\frac{\partial}{\partial x_i}(u_i \varphi) - \frac{\partial \mathcal{R}_{\varphi,i}}{\partial x_i} + S_\varphi \tag{1}$$

where $\mathcal{R}_{\varphi,i}$ is the sub-grid scale scalar flux vector. The volumetric term is determined by

$$S_\varphi = -a u_d \varphi \tag{2}$$

where u_d is the deposition velocity and a is the leaf are density of the tree canopy. The deposition velocity is a conductance term that captures the aerodynamic, laminar boundary layer and surface resistances to pollutant deposition. Values of u_d vary significantly between species, pollutants and numerous other factors. There is currently insufficient data to produce a robust parameterisation (Janhäll, 2015). Values vary significantly in the literature but are generally less than 0.01 m s^{-1} for most pollutants and tree species (Santiago et al., 2017). Recent wind tunnel experiments by Wang et al. (2019) indicate significantly higher values (~10 times) are also possible under certain conditions for the deposition of particulate matter.

Volumetric terms are also applied to the constitutive equations for wind velocity u_i, specific humidity q_v and temperature T. The sink term representing the drag imposed by the tree canopy on the surrounding flow field is well established

$$S_{u_i} = -a C_d |u| u_i. \tag{3}$$

$|u|$ is the absolute wind speed and C_d is the drag coefficient, which typically varies from 0.1 to 0.3 depending on the tree species (Buccolieri et al., 2018).

The volumetric terms for specific humidity S_{q_v} and temperature S_T allow for complex thermal effects to be captured while avoiding the need to solve for leaf temperatures. The tree model does this by

simplifying the radiative budget into a one-dimensional problem with the tree canopy broken down into a set of horizontal slices. The tree model lumps upwelling and downwelling shortwave and longwave radiation in a single net all-wave radiation term Q^* and assumes that all exchanges occur vertically. Incident net radiation is considered from above the canopy onto the tree crown. The trees are assumed to absorb radiation according to the Beer-Lambert law with a constant extinction coefficient α. Enthalpy conservation in each grid cell containing part of the tree canopy then stipulates that the radiation absorbed by the leaves has to be emitted either as a sensible heat flux at the local leaf surface Q_{Hl} or as a latent heat flux at the local leaf surface Q_{El}. These two terms interact with the surrounding air as volume sources of the form

$$S_{q_v} = a\frac{Q_{El}}{\rho L_v}, \qquad S_T = a\frac{Q_{Hl}}{\rho c_p} \tag{4}$$

where ρ is the air density, L_v is the latent heat of vaporisation, and c_p is the heat capacity of the air.

The remaining net radiation below the tree then interacts with the ground. Here, the objective hysteresis model (OHM) is used to determine how much of the remaining radiation is stored in the ground and how much is emitted as sensible heat (Grylls and van Reeuwijk, 2021). Unshaded surfaces are assumed to receive the same incident net radiation as the tree crowns. The OHM is used to obtain the corresponding sensible heat flux for all unshaded surfaces. This process is followed both for situations with and without trees to facilitate a fair comparison between the two cases. Details of these sources and a validation of this tree model can be found in Grylls and van Reeuwijk (2021).

2.3. Case description

Simulation set-ups were devised that facilitate the impact of trees on air quality in urban areas to be systematically investigated. The simulations outlined below enable converged statistics to be obtained over a physically representative, generalised case of an infinite street canyon with traffic emissions, with and without trees, and under both neutral and convective conditions.

2.3.1. Trees in infinite street canyons

Infinite canyons are modelled with an aspect ratio of 1 and a building height of 32 m (see Fig. 1). This configuration without trees has been studied extensively in the literature (Buccolieri et al., 2011; Gromke and Ruck, 2012; Aboelata, 2020) and provides a platform through which to explore the sensitivity of tree's combined effects to other key parameters.

The base case tree set-up is composed of two trees on the wind- and lee-ward sides of each canyon as shown in Fig. 1a and b. The idealised forms of the tree canopies provide a set-up that 1) facilitates a simplified configuration for analysis and 2) has been used widely in existing studies of urban trees (Salim et al., 2011; Li and Wang, 2018). Similarly the tree parameters (leaf area density, leaf size etc.; see Table 1) are assigned homogeneously throughout the canopies (although the tree model supports non-homogeneous distributions).

The main simulation parameters are outlined in Table 1. Values are assigned that are typical of large urban trees following the literature (Jones, 2013; Buccolieri et al., 2018), e.g. a deposition velocity u_d of 5×10^{-3} m s^{-1} (similar values have been applied to separate studies of NO_x, PM2.5 and PM10; Buccolieri et al., 2018), a leaf area density a of 1 m^2 m^{-3} and a leaf size l of 0.15 m.

2.3.2. Statistically stationary neutral and convective boundary layers

Four simulations are performed: neutral (N), neutral with trees (NT), convective (C) and convective with trees (CT). A friction velocity of 0.3 m s^{-1} is enforced in all four simulations using a constant pressure gradient forcing.

As implied by their name, the neutral cases N and NT consider the effect of trees in absence of buoyancy effects. The radiative conditions defined for the convective cases C and CT are that of a summer's day at noon with low cloud cover (conducive of strong net irradiation at the urban surface and a low zenith angle; these conditions are approximated following the parametrisations outlined in CERC, 2001; Grylls and van Reeuwijk, 2021). $q_{v,0}$ and θ_0 indicate the assigned values for uniform initial profiles of water vapour specific humidity and potential temperature.

Incorporating the trees' integrated effects on momentum, temperature, moisture and pollutants necessitates careful consideration in terms of the applied boundary conditions. Periodic boundary conditions are applied in the spanwise directions for momentum, temperature and moisture such that a statistically stationary and horizontally homogeneous urban boundary layer (UBL) can be obtained.

For neutral cases N and NT, turbulence production is due to shear

Table 1
Environmental and tree parameters used in the four simulations of the trees in infinite canyons study: neutral (N), neutral with trees (NT), convective (C) and convective with trees (CT). The trees have a leaf area density $a = 1.00$ m^2 m^{-3}, leaf size $l = 0.15$ m and deposition velocity $u_d = 0.005$ ms^{-1}. r_s represents the stomatal resistance.

Sim.	u^*	$q_{v,0}$	θ_0	Q_a^*	$\frac{dQ_a^*}{dt}$	r_s	α
	[m s^{-1}]	[kg kg^{-1}]	[K]	[W m^{-2}]	[W m^{-2} hr^{-1}]	[s m^{-1}]	[-]
N	0.30	–	–	–	–	–	–
NT	0.30	–	–	–	–	–	–
C	0.30	–	288.15	450.20	15.47	–	–
CT	0.30	0.00735	288.15	450.20	15.47	200	0.40

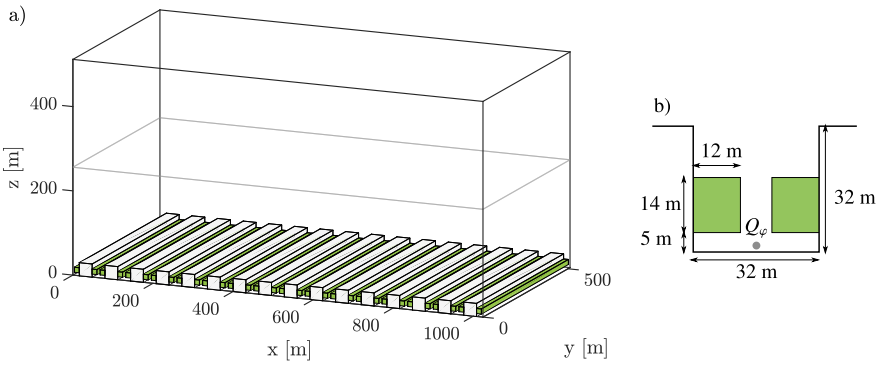

Fig. 1. a) Domain and canopy set-up applied for the simulations of trees in infinite street canyons (the grey line represents the domain height used for the neutral simulations). b) Diagrammatic representation of the tree configuration within each street canyon.

only and is therefore predominantly local: it is dissipated at the same height it is produced. Consequently, a limited domain height covering the roughness sublayer will suffice for the simulations and as such the domain height in simulations N and NT is set to 256 m (indicated by the grey line in Fig. 1a).

For the convective cases C and CT, turbulence production will also be due to buoyancy which is principally a non-local process: the turbulence will not be dissipated where it is produced. This necessitates a sufficiently large domain height h. Using the findings of Grylls et al. (2020), a domain height, h, is set that is greater than half the predicted convective boundary layer (CBL) height ($h \geq h_C/2$)) and five times the relevant Obukhov length ($h \geq 5\ \max(|L|, |L_{\min}|)$) in simulations C and CT. Using the meteorological conditions approximated for the convective, no trees base case: $h_C \approx 1024$ m (estimated using mesoscale parametrisations; Batchvarova and Gryning, 1991; CERC, 2001) and L and $L_{\min}$ are -14.2 m and -50.6 m respectively (Businger, 1973; Grylls et al., 2020). A domain height of 512 m is therefore defined for the convective cases. The grid is stretched in the z-direction in simulations C and CT such that the grid size is the same as simulations N and NT but a resolution of 1 m is retained up to $z = 50$ m. The maximum vertical cell size is 3.21 m at the top of the domain.

The streamwise length of the domain is set to $2h$ (1024 m) for these two convective simulations resulting in a relatively large domain for an investigation of infinite canyons (the same streamwise length is defined for the neutral simulations to enable a direct comparison of the developing pollutant fields). The grid size of all simulations is $512 \times 256 \times 256$.

Simulations are run up until the UBL has reached a steady-state. Statistics are then taken with a sampling time of 2 s and sampling period of 6000 s or larger. In order to produce a statistically steady state also for the convective boundary layer, a constant heat flux is imposed at the top of the domain to reproduce the expected linear heat flux profile of a convective boundary layer up to the top of the modelled domain (Grylls et al., 2020); its value is set to half of the net heat flux into the fluid domain from the unshaded surfaces, shaded surfaces and tree canopies combined. This calculation is made by integrating over the relevant areas and volumes: $\varphi_{\theta,h} = (2\ A)^{-1}\left[\int \varphi_{\theta,u} dA + \int \varphi_{\theta,s} dA + \int S_\theta dV\right]$ (where A is the horizontal extent of road and roof top surfaces within the domain). A uniform volumetric cooling term is applied throughout the domain to account for the resulting imbalance in the total heat flux in and out of the domain and to enforce the expected linear profile of turbulent heat flux in the CBL: $R = -\varphi_{\theta,h}/h_M$ (where h_M is the vertical size of the domain weighted by the masking matrix over the buildings).

In a typical stationary CBL, one expects a flux of moisture from the 'surface', a relatively uniform profile of humidity over the convective mixed-layer and a flux of the same sign over the entrainment zone where moisture is transferred to the free atmosphere above (Stull, 2012). To replicate these expected profiles in uDALES, the moisture flux at the top of the domain is defined to equal the integrated flux from the tree canopies $\varphi_{q_v,h} = \left[\int S_{q_v} dV\right]/A$ (resulting in a uniform profile of the turbulent moisture flux; equivalent to method *ii* in Grylls et al., 2020).

2.3.3. Pollutant transport

A pollutant line source Q_φ is placed in the centre of each canyon at a height of 0.5 m (Fig. 1b). Contrary to the velocity, potential temperature and humidity fields, the lateral boundary conditions for concentration cannot be assumed to be homogeneous. Indeed, this would imply that there is a region upwind with identical emissions rates over which the pollutant has mixed across the entire boundary layer depth. The problem with this assumption is that, depending on e.g. the wind speed and rate of vertical mixing, it implies identical upwind emissions for tens of kilometres or more.

The validity of this homogeneity in the emissions can be understood by considering the time and length scales over which mixing would need to occur. The eddy turnover time is a characteristic time scale that is representative of this mixing process Stull (2012). $\tau \approx h/u^*$ or $\tau \approx h/w^*$ for neutral or freely convective conditions respectively where $w_* = \left[(g/\theta_0) h \varphi_{\theta_v,0}\right]^{1/3}$ is the Deardorff scale. Substituting the values associated with simulations N and C and using $h = 512$ m for both calculations, the corresponding eddy turn-over times are 1707 s and 380 s respectively. Given a typical wind speed of 5 m s^{-1} these timescales relate to corresponding upwind distances of 8.5 km and 1.9 km under neutral and convective conditions respectively. The assumption for stationarity in the pollutant field is therefore more reasonable under convective conditions than for neutral atmospheric conditions.

In order to allow a one-by-one comparison of the urban pollution under both neutral and convective conditions, inflow-outflow boundary conditions are used for the scalar fields across all simulations. This allows the pollutant fields to develop in the streamwise direction in a UBL which is otherwise statistically stationary. A uniform background concentration can be assigned at the inlet boundary to represent the background air quality.

In this study, we study the effect of trees on air quality via a setup that uses superposition of background concentration and local emissions to construct realistic scenarios encountered in urban settings, e.g. the case of NO_x which is predominantly governed by the local emission sources, and PM2.5, whose presence is generally dominated by the background concentration. In order to represent both scenarios in a single simulation, the background concentration φ_b is solved independently from the emitted concentration φ_e. Specifically, we set:

$$\varphi_b: \quad \varphi_b(0, y, z) = 1, \quad Q_{\varphi_b} = 0, \tag{5}$$

$$\varphi_e: \quad \varphi_e(0, y, z) = 0, \quad Q_{\varphi_e} = 1. \tag{6}$$

That is, the background concentration φ_b is assigned a uniform profile at the inflow boundary but without emissions in the canyons. Conversely, the emitted concentration is 0 at the inflow boundary and sets a unity scalar source in the canyons. Given the linearity of the scalar conservation equation (1) and the volumetric deposition term (2), any pollution scenario can be reproduced using the superposition principle

$$\varphi = c_1 \varphi_b + c_2 \varphi_e \tag{7}$$

where c_1 and c_2 are arbitrary weights. This method allows for depositional effects to be explored for scalars that are emitted locally, remotely or a mixture of both from a single simulation. It should be noted that (7) is valid only for passive scalar scenarios; the scalar transport equation is non-linear for simulations involving chemical reactions (e.g. Grylls et al., 2019).

3. Results

3.1. Flow field

Figs. 2 and 3 show the variation in flow profile and velocities within the domain for the four simulated cases. Focussing first on the difference between the neutral and convective cases without trees, it is apparent that the wind speed above the UCL is higher for the neutral case in both of these figures. The friction velocity is matched across these simulations and the large domain-size turnovers present in the convective case result in increased drag that, given the same flow forcing, results in lower bulk wind speeds. The enhanced mixing in the convective UBL also results in practically uniform velocity profiles above the UCL, unlike the neutral case where the wind has a logarithmic profile.

Despite the reduced wind speeds above the UCL, simulation C exhibits higher in-canyon velocities than simulation N (canyon-average absolute wind speed of 0.55 m s^{-1} as opposed to 0.48 m s^{-1} in the neutral case; 14% higher). The canyon vortex in this simulation is consistent with the thermally reinforced recirculation regime identified in the study of bottom heated canyons of Kim and Baik (2001). The

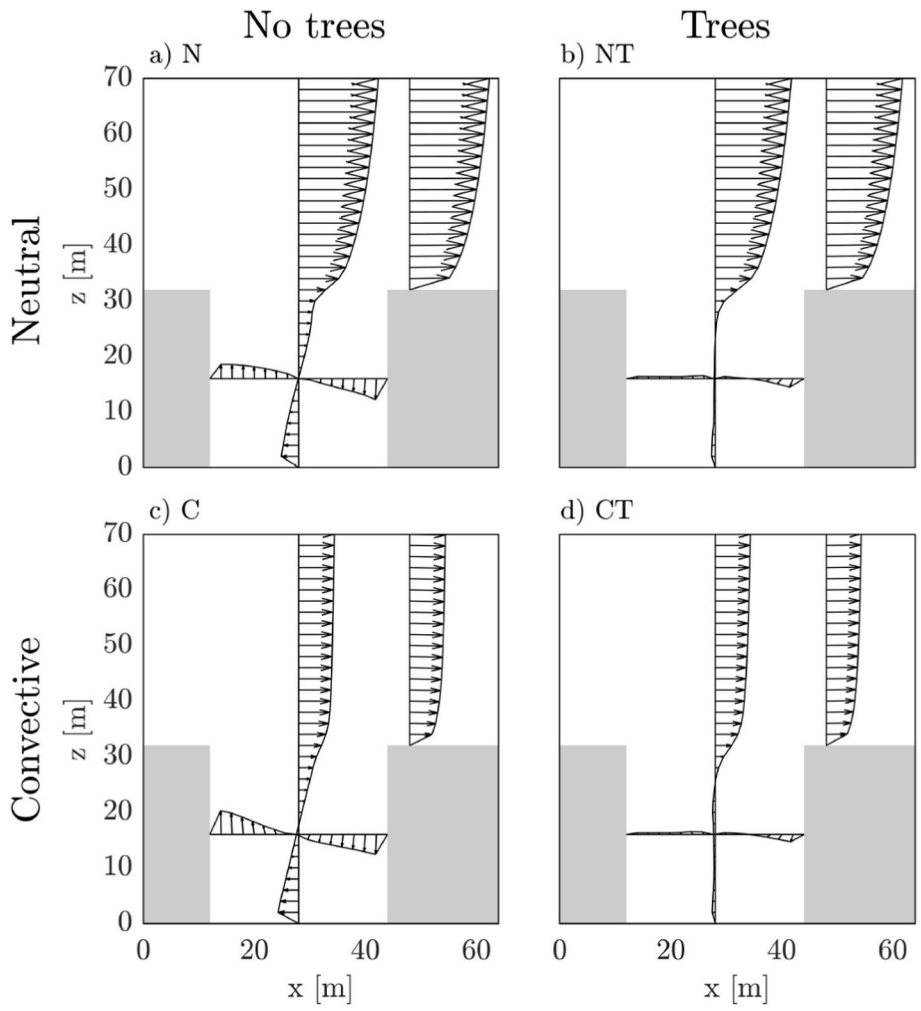

Fig. 2. Quiver plot of the time- and spanwise-averaged flow fields for the a) neutral (N), b) neutral with trees (NT), c) convective (C) and d) convective with trees (CT) simulations.

streamlines at the top of the canyon in Fig. 3c curve upwards over the top of the canyon (a phenomenon discussed by Allegrini et al., 2014) and this enhanced vortex diameter further illustrates the effect of buoyancy on the canyon vortex (shown to weaken the shear layer in Li et al., 2010). Given equal wind speeds above the UCL, the convective case would exhibit significantly higher in-canyon velocities in comparison to the neutral case (the flow reinforcement has acted to balance out the relative wind speed deficit in these two simulations). Similar effects have been exhibited for ground heating of canyons with different aspect ratios (a regime change due to heating was only exhibited for an aspect ratio of 0.5; Li et al., 2012).

The effect of trees is to reduce the velocities inside the canyons for both the neutral and convective cases. This observation is to be expected as the drag force exerted by the tree leaves results in lowered in-canyon velocities (canyon-averaged absolute wind speeds reduced by 62% and 72% with trees for neutral and convective conditions respectively). The blocking effect of the trees is shown to be significant and of similar magnitude in both simulations NT and CT. Fig. 3b and d indicate that the presence of trees has also significantly altered the canonical canyon vortex exhibited by simulations N and C. The centre of the vortex is moved significantly as the top of the windward tree crown acts to inhibit flow down the facade of the windward building in both simulations. A smaller secondary vortex also forms in the lower leeward corner of the canyon in both simulations NT and CT. Whilst the positions of the centres of these vortices are similar for both neutral and convective conditions, there is an apparent difference in the structure of the vortices as shown in Fig. 3b and d. The streamlines illustrate that the flow structure is comparatively stretched in the horizontal direction and that there is a distinct shift in the flow over the leeward tree canopy in simulation CT. This difference illustrates that buoyancy has a non-negligible effect on the flow within the canyon although the similarities in terms of the vortex centres suggest that it is still secondary to the direct effects of drag. The reduced wind speeds in the canyons result in larger velocity deficits across the shear layer. This change therefore directly affects one of the prevalent velocity scales that defines this transfer between the canyon and overlying boundary layer (Salizzoni et al., 2011).

3.2. Temperature and humidity

Fig. 4 shows the spanwise and time-averaged potential temperature fields for the two convective simulations. Fig. 4a clearly shows the increased temperatures arising from the bottom heating of the canyon. The reinforced canyon vortex results in efficient mixing within the canyon which is evident from the relatively homogeneous temperature field above the lowest 5 m of the canyon. The effect of trees is to redistribute and alter the sources/sinks of buoyancy within the canyon. Fig. 4b illustrates increased temperatures at the tree crowns tops (smaller than the maximum temperature shown in simulation C) and decreased temperatures down through the canopy and at pedestrian level beneath. The canyon-averaged temperature in simulation CT is 0.23 K cooler than in simulation C and the pedestrian-averaged

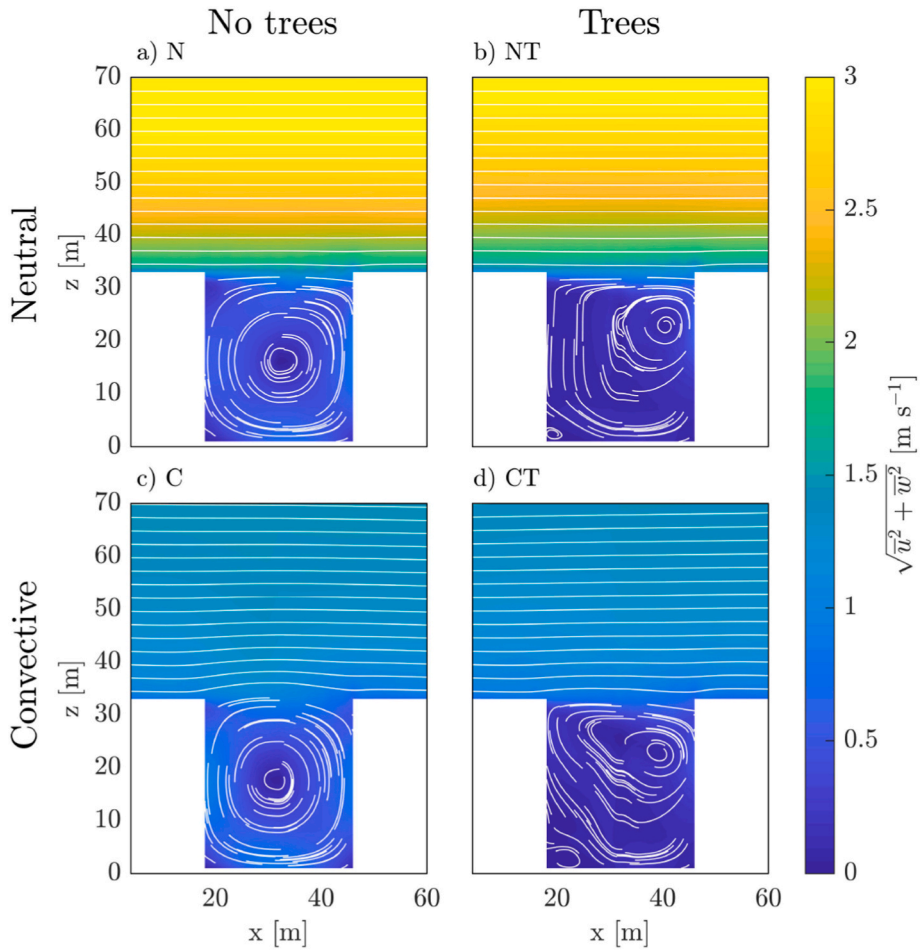

Fig. 3. Streamlines and plots of the time and spanwise averaged flow field and wind speed for the a) neutral, b) neutral with trees, c) convective and d) convective with trees simulations.

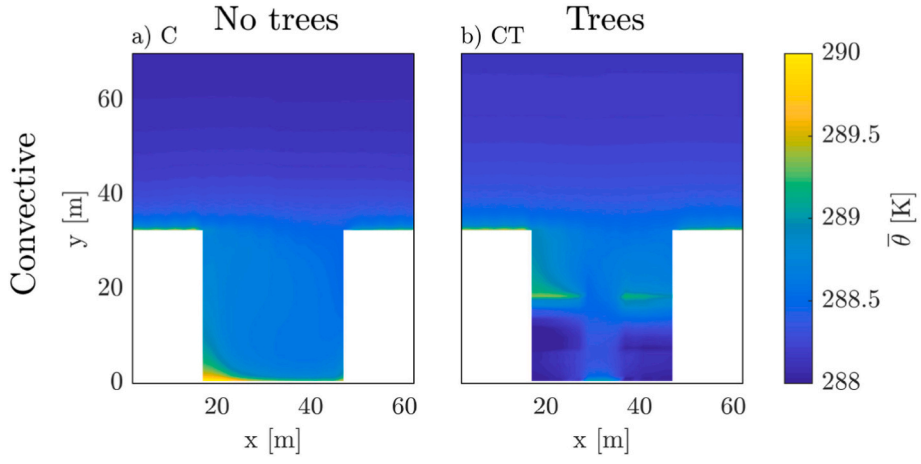

Fig. 4. Time- and spanwise-averaged potential temperature for the a) convective (C) and b) convective with trees (CT) simulations.

temperature (at $z = 1.5$ m) is 0.83 K cooler. These results are consistent with the temperature difference found in field studies (Bowler et al., 2010). In terms of pedestrian thermal comfort, the cooling effect of the trees is much larger as a result of the direct benefits of tree shading on a pedestrian.

For the relatively strong radiative conditions ($Q_a^* = 450$ W m^{-2}) and leaf area index (leaf area per unit ground; $d = 12$) modelled in this study, the heat flux from the shaded surfaces $\varphi_{Q_{H,s}}$ is 284 W m^{-2} (166 W m^{-2} less than the unshaded surfaces). This results in a cooling power per unit length of the street canyon of -3984 W m^{-1} due to the tree shading effect.

Fig. 5 displays the spanwise and time-averaged volumetric sources and sinks of the water vapour specific humidity, temperature and the emitted and background scalar components. Fig. 5d illustrates that the tree canopy itself acts as both a source and sink of sensible heat, as a heat source at the canopy top and a sink towards the bottom of the canopy

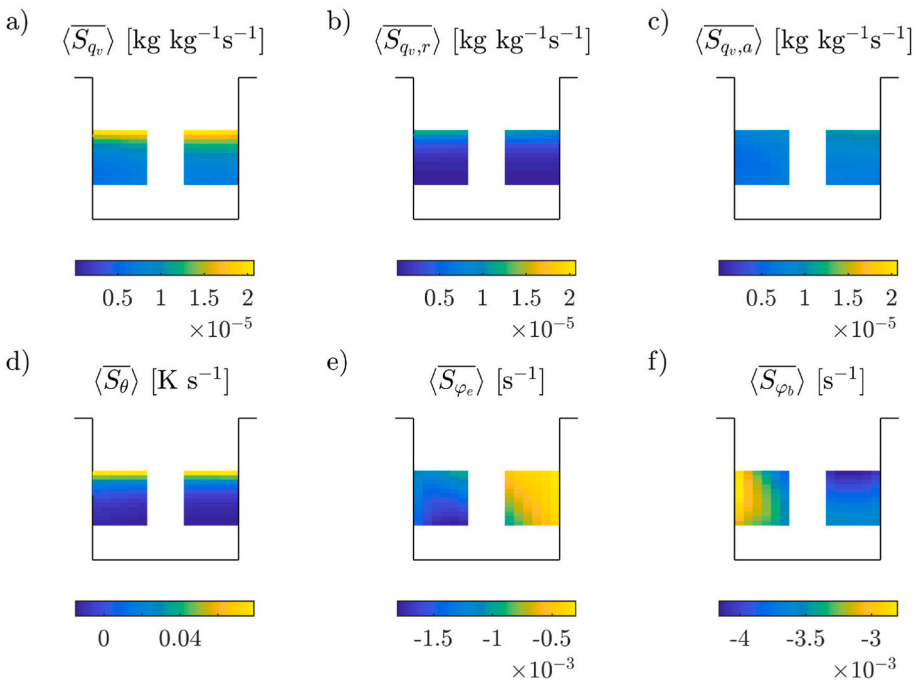

Fig. 5. Time- and spanwise-averaged volumetric sources and sinks of a) water vapour specific humidity, b) the radiative component of water vapour specific humidity, c) the advective component of water vapour specific humidity, d) potential temperature, e) the emitted component of the pollutant field and f) the background component of the pollutant field for the tree canopies in simulation CT. The 8th canyon from the inlet boundary is used for S_{φ_e} and S_{φ_b}.

(following a similar trend to that exhibited in Manickathan et al. (2018)). The total average sensible heat flux from the two tree canopies to the surrounding air is 2684 W m^{-1} (112 W m^{-2} average per unit ground area). Following the tree regimes identified in Grylls and van Reeuwijk (2021), the trees therefore have a net tree cooling (*NTC*) coefficient of 0.12, indicating that the net sensible heat flux is positive but smaller than would be the case if there were no trees. The tree cooling ratio *TCR* is −0.73, which illustrates that tree shading is the dominant mechanism for cooling over transpirational cooling for this case. The trees therefore lie in the 'Net reduction, shading dominated' tree cooling regime under these conditions.

The volumetric sources of moisture from the tree canopies are displayed in Fig. 5a, b and c (broken down into radiative and advective components). The total source of water vapour specific humidity is 0.003 kg kg^{-1} m^{-1} s^{-1} of which 73% is attributed to the advective component of the latent heat flux. It is important to note that the proportion due to the available energy at the leaf surface is non-negligible and that the latent heat flux is not spatially homogeneous throughout the tree canopy as has been assumed in previous studies. The advective component is shown to be relatively uniform throughout both tree canopies (in comparison to total the range of S_{q_v} between both canopies) and the radiative component is shown to be predominantly determined by the decay of radiation in the z-direction.

The tree's effect on buoyancy can be understood by the change in virtual potential temperature, which is a function of both potential temperature and the water vapour specific humidity (see Grylls, 2019; Suter et al., 2021). The maximum and minimum volumetric source/sink terms of virtual potential temperature from the tree canopies in simulation CT are 0.0795 and −0.017 K s^{-1} respectively. The magnitude of the volumetric source of water vapour (maximum source term 2.1× 10^{-5} kg kg^{-1}s^{-1}) has a negligible effect on these values indicating that the latent heat flux from tree canopies does not directly affect the buoyancy of the surrounding air. The distribution of S_θ is a good indicator of the buoyancy sources introduced by the tree canopy. This source therefore acts to alter the flow field in terms of the positive buoyancy source at the canopy top and the negative source towards the bottom. The streamlines in Fig. 3d illustrate the buoyancy effect on the flow structure within the canyon.

The case of an infinite canyon and horizontally homogeneous tree canopies is not conducive of the 'oasis' effect (Akbari et al., 1990; Grimmond and Oke, 1991) as the relatively low rates of vertical exchange lead to correspondingly higher values of specific humidity within the UCL. As the trees simultaneously act to cool the surrounding air, this case set-up can result in increased relative humidities and therefore vapour pressure deficits (in comparison to the initial values; canyon-average relative humidity of 72.3% in simulation CT). The generally low wind speeds present in the canyon in simulation CT also act to reduce the average aerodynamic resistance leading to reduced latent and sensible heat fluxes. One may expect the latent heat flux and therefore transpirational cooling to be relatively increased in more complex morphologies and with sparser tree canopies. Further work is required to gain a more complete understanding of the transpirational and shading effects of trees (encompassing the entire parameter space) but these results suggest that this tree model is a good tool with which to do this.

3.3. The effect of trees on local and background sources of air pollution

Fig. 6 shows the streamwise development of the emitted passive scalar field, φ_e, for simulations N and C. The combination of higher wind speeds and less vertical mixing in the neutral case results in significantly different downwind dispersion characteristics. The pollutant plume can be seen to mix over the height of the domain after approximately 600 m for the convective case in Fig. 6b whereas it reaches a height of only 100 m under neutral conditions in Fig. 6a, consistent with the discussion of eddy turnover times in Section 2.3. The differences exhibited by the neutral and convective cases illustrate the difficulties in directly comparing pollution dispersion under different atmospheric stabilities and simultaneously highlight the importance of capturing thermal effects in studies of urban pollution dispersion. The canyon-averaged pollutant concentrations increase in the streamwise direction in both of these simulations as a result of the increasing above-canyon concentrations and subsequent detrainment (5.5% and 6.2% larger in the fifteenth canyon from the inlet boundary in comparison to the first for

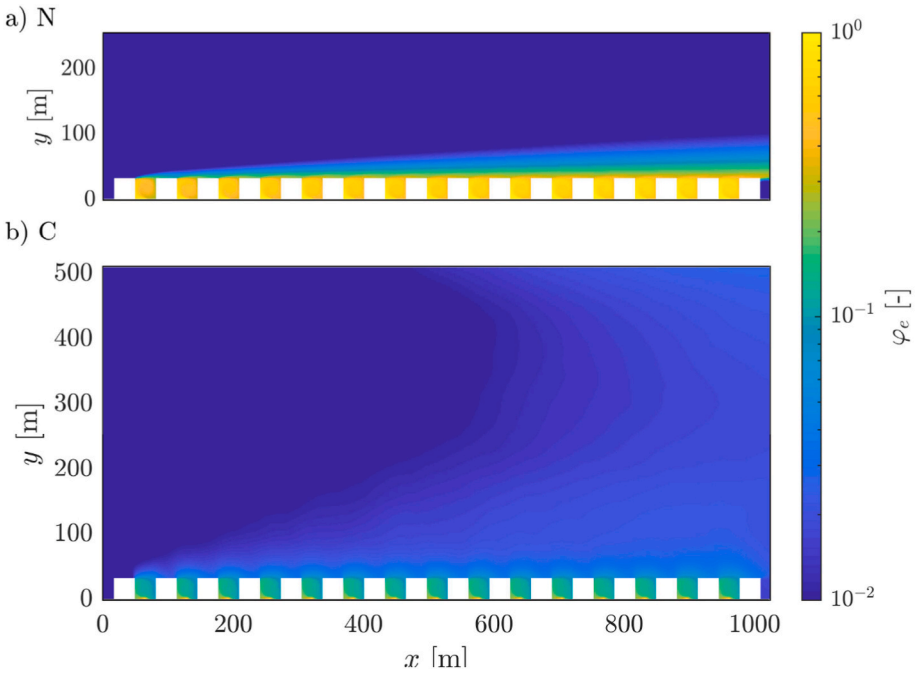

Fig. 6. Time- and spanwise-averaged emitted components of the pollutant concentration in the a) neutral and b) convective simulations.

simulations N and C respectively). The 8th canyon from the upwind side of the domain is used for the following analysis.

Fig. 7 shows the resulting time- and spanwise-averaged pollutant fields of the emitted scalar φ_e and background scalar φ_b for the four base case simulations. We note that φ_b is only shown for the simulations with trees as it is uniform without trees. The difference between air quality under neutral and convective conditions is reiterated in this figure by the requirement to use different colour bars to illustrate the distribution of pollutants within the canyon. The canyon-averaged concentration in simulation N is about 5 times larger than the canyon-averaged concentration in simulation C for the emitted scalar φ_e. The reason for the magnitude of this difference is that whilst the friction velocities are matched in these simulations (which is the dominant scaling in defining vertical exchange in the neutral case), the Deardorff velocity scale is also an important scaling under convective conditions. For the CBL modelled here, the Deardorff velocity scale is 1.35 m s^{-1} which is significantly larger than the specified friction velocity ($u^* = 0.3$ m s^{-1}). The Obukhov length is -14.2 m, which also indicates the dominance of buoyancy in

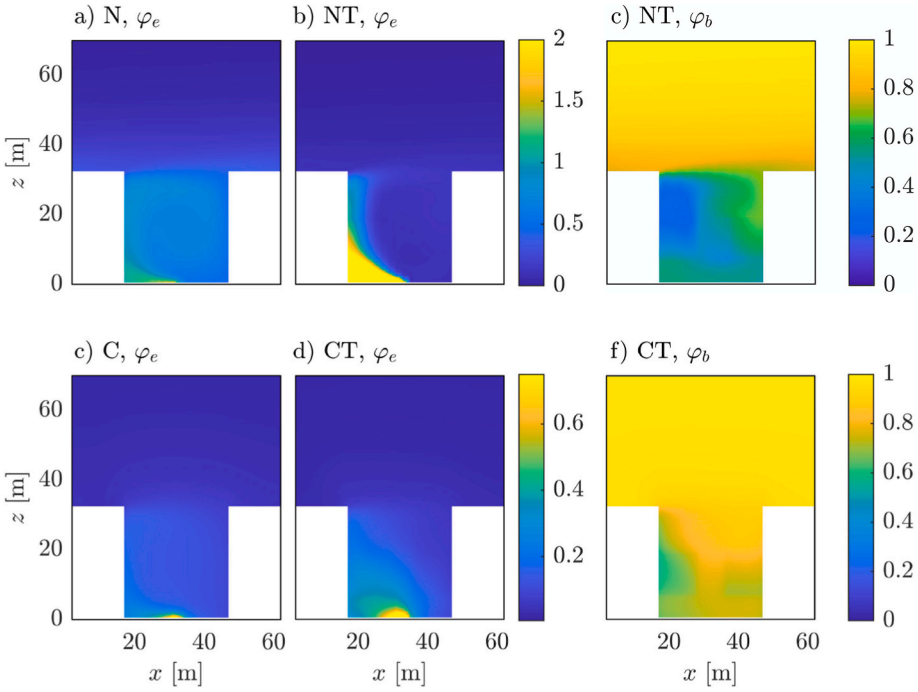

Fig. 7. Time- and spanwise-averaged pollutant concentrations for the emitted scalar φ_B and background scalar φ_b in the eighth canyon from the inlet boundary. a) φ_B for neutral conditions without trees (colorbar in figure b), b) φ_e for neutral conditions with trees. c) φ_b for neutral conditions with trees, d) φ_e for convective conditions without trees (colorbar in figure e), e) φ_e for convective conditions with trees. f) φ_b for convective conditions with trees.

the modelled CBL (the minimum Obukhov length is −50.7 m; Businger, 1973). The effect of this scaling is evident in the measured exchange velocities u_e, which are 0.04 and 0.21 m s^{-1} for simulations N and C respectively (Table 2). The exchange velocity represents the rate at which pollutants are exchanged between the street canyon and the atmosphere aloft (the 'breathability' of the street canyon) and was calculated using the emitted scalar $\overline{\varphi}_e$ as Barlow et al. (2004); Salizzoni et al. (2009).

$$u_e = \frac{1}{W\langle\overline{\varphi}_e\rangle_c}\int_{x_0}^{x_0+W} \overline{w}(x,H)\overline{\varphi}_e(x,H) + \overline{w'\varphi'_e}(x,H)\mathrm{d}x \tag{8}$$

where x_0 is the start of the eighth canyon, H and W are the canyon height and width respectively, and $\langle\overline{\varphi}_e\rangle_c$ is the canyon-averaged concentration. The background concentration is zero for the emitted scalar so does not appear in the expression above. The magnitude of these exchange velocities is consistent with the empirical parametrisations applied within SIRANE that, using the modelled boundary layer properties, predict corresponding values of 0.08 and 0.17 m s^{-1} (calculated as a function of the parametrically defined standard deviation in vertical velocity; Soulhac et al., 2011).

Fig. 7b and d illustrate the combined drag, buoyancy and deposition effects of trees on the emitted scalar field φ_e. Both simulations with trees exhibit higher concentrations on the leeward side of the canyon. Simulation NT shows a particularly large hotspot of pollution at pedestrian level on the this side where a small secondary circulation was shown to exist in Fig. 3. The increased concentrations are a direct result of the drag imposed on the flow within the street canyons. In simulation NT the depositional effects of the tree are evident in that the concentration on the windward side of the canyon is lower than in comparison to simulation N. The position of the tree canopy in this base case scenario is such that the majority of the emissions flow through the windward tree canopy relatively quickly and before they are significantly diluted. A large proportion of the emitted pollutant is deposited through this process in simulation NT. The review of Abhijith et al. (2017) highlights a number of studies that found the same asymmetry when studying infinite canyons with a perpendicular wind angle of incidence. The same asymmetrical effect is apparent between simulations C and CT but to a lesser extent. The buoyancy sources in simulation CT were shown to result in a different flow structure and it is suggested that more of the pollutant is transported closer to the centre of the canyon and therefore not through the windward tree canopy. The sink of φ_e in simulation CT is displayed in Fig. 5. The largest sink of pollutant is in the leeward tree canopy and towards the centre of the canyon, which agrees with this hypothesis. The increased vertical exchange in the convective simulation also means that the emitted component of the scalar field has a lower residence time within the canyon. This difference between neutral and convective conditions significantly alters the canyon-averaged effects of the trees.

The effect of trees on the background concentration is shown in Fig. 7d and f. Here, the situation is the exact opposite of when the emissions are inside the canyon: in this case, the polluted air is transported into the canyon via the canyon top, causing polluted air to descend on the windward side. As it moves through the trees, the air is filtered, causing the air quality on the windward side to be worse than on the leeward side. The difference between the neutral and convective case is limited. The stonger interaction with the atmosphere under convective conditions causes a larger flux of polluted air into the canyon and thus higher pollution levels than under neutral conditions.

This positioning aspect of using trees and green infrastructure to mitigate poor air quality has been discussed in e.g. Morakinyo et al. (2017). If the pollutant field is generally at a higher concentration and less associated with direct emissions this effect is diminished. Fig. 5f shows the volumetric sink of the background component of the modelled pollutant field. The largest sink of pollution is on the windward tree canopy however the magnitude of the sink term is generally more uniform between the two canopies than the sink of the emitted component. The removal of background air pollution is therefore more efficient than of the emitted pollutant field as the proximity to the emissions source and local transport of the emissions is irrelevant. The same effect therefore applies to trees in quieter streets and parks as discussed in Section 5.

It is important to note that generally the most harmful levels of pollutants are associated with direct emissions and hotspots close to specific emission sources. It is therefore necessary to study the absolute reduction in pollutant levels as well percentage terms. However, the application of the weighting factor in this study has highlighted a phenomena of urban trees that has hitherto rarely been considered. As in Section 3.2, further work is required to gain a more holistic understanding of the role of trees in urban air quality (encompassing the full parameter space) however these results again reiterate that the minimal tree model and the roadside-background concentration ratio present useful tools with which to do this.

Table 2
Time- and canyon-averaged quantities and exchange velocities u_e in the four simulations of the trees in infinite canyons study: neutral (N), neutral with trees (NT), convective (C) and convective with trees (CT). Averages are obtained for the eigth canyon. The calculation of u_e is explained in Section 4.

Sim.	$\langle\overline{\theta_v}\rangle_c$ [K]	u_e [m s^{-1}]	$\langle\overline{\varphi_e}\rangle_c$ [-]	$\langle\overline{\varphi_b}\rangle_c$ [-]	$\langle\overline{\mathrm{NO_x}}\rangle_c$ [μg m^{-3}]	$\langle\overline{\mathrm{PM2.5}}\rangle_c$ [μg m^{-3}]
N	–	0.042	0.705	1.000	95.150	12.455
NT	–	0.016	0.571	0.492	62.846	6.396
C	288.709	0.213	0.144	1.000	54.899	11.774
CT	288.494	0.114	0.196	0.768	48.317	9.152

3.4. The effect of trees on NO_x and PM2.5 concentrations

As discussed in Section 2.3, a weighting c_1 and c_2 can be applied to the background (φ_b) and emitted (φ_e) scalar fields respectively to study the effects of trees on different pollutants or under different emission rates. The example applied in this analysis is that of capturing 'effective' roadside NO_x and PM2.5. NO_x concentrations in cities are often dominated by road transport emissions and as such one typically expects much larger values close to busy roads than in quieter roads or parks (Oke et al., 2017; Grylls et al., 2019). PM2.5 is also associated with vehicular emissions but due to a combination of other source attributions and different chemical interactions, it generally exists more homogeneously within the urban boundary layer. London-wide air quality data can be used to provide reference values of the roadside and background concentration ratios that characterise this effect. The average roadside and background concentrations in London for NO_x were 103.7 μg/m^3 and 44.6 μg/m^3 respectively (using monthly averages taken at 12:00 over a period of a year; King's College London, 2019). For PM2.5, the average roadside and background concentrations were 12.6 μg/m^3 and 11.6 μg/m^3, respectively over the same time period.

Since φ_b uses a unit concentration as its upwind boundary condition, the weight c_1 for the background concentration in (7) is set to be equal to the background concentration itself. The weight c_2 for the emitted scalar, which controls the strength of the emission source Q_φ is obtained by averaging (7) at pedestrian level across the canyon, which results in

$$\langle\varphi\rangle_p = c_1\langle\varphi_b\rangle_p + c_2\langle\varphi_e\rangle_p \tag{9}$$

where $\langle\cdot\rangle_p$ denotes averaging across a canyon at pedestrian height. Recognising that the left-hand side is a typical roadside concentration and that $\langle\varphi_b\rangle_p$ and $\langle\varphi_e\rangle_p$ follow from the simulation data, the only unknown in the equation above is c_2.

In the analysis below, we will assume that the average roadside and background concentrations were measured under neutral conditions in a canyon without any trees present, so the data from simulation N can be used to determine $\langle\varphi_e\rangle_p$ and $\langle\varphi_b\rangle_p$. This results in weights for NO_x of $c_1 =$

44.6×10^{-6}, $c_2 = 71.7 \times 10^{-6}$ and the weights for PM2.5 of $c_1 = 11.6 \times 10^{-6}$, $c_2 = 1.2 \times 10^{-6}$. These weights will be applied to all other simulations in order to investigate the effects of atmospheric stability and trees on the canyon-average and pedestrian-level concentrations under conditions that are identical otherwise.

Shown in Fig. 8a is the NO_x concentration for the neutral simulation with trees. As the NO_x concentration is dominated by emissions inside the canyon, the behaviour of φ_e dominates, and a trapping of the pollutant causing concentrations that are substantially higher than without trees, particularly on the leeward side, is observed. The expected roadside NO_x concentrations, based on the pedestrian-level average over canyon 8, are shown for all four scenarios in Fig. 8c in the labels denoted with "ped". It is clear that under neutral conditions, when the interaction with the atmosphere is relatively weak, the effect of trees is substantial and is detrimental to air quality. This is particularly true for the leeward side of the canyon, where the local concentrations are substantially larger. Interestingly, when considering the average concentration over the entire canyon, denoted with "can", the average air quality actually improves. In this case, the trapping of pollutant underneath the trees is substantial, which explains the slightly counterintuitive results between the canyon-average and pedestrian-level-averaged results. The effect of trees on the air quality inside the canyon is much smaller under convective conditions, since the interaction with the atmosphere, quantified by the exchange velocity u_e (Table 2), is much stronger than for the neutral case which causes much lower concentrations inside the canyon, and therefore also a smaller impact of the trees on air quality. This is due to a reduced residency time of the pollutants in the canyon, which is of the order of H/u_e. For this case, both the canyon-averaged and pedestrian-level-averaged concentrations reduce as the result of having trees.

Fig. 8d shows the PM2.5 concentration for the neutral simulation with trees. Here, the concentrations are dominated by the background levels and thus the behaviour of φ_b. The absence of strong emissions inside the canyon means that the trapping effect underneath the tree is much less significant, and the trees are beneficial for air quality across the board. This is evident in Fig. 8f, which shows canyon-averaged and pedestrian-height-averaged PM2.5 concentrations for the four simulations. Here, trees are beneficial in both circumstances, reducing the pedestrian-level-averaged concentrations by 30% (N) and 25% (C) relative to the no-tree case. Moreover, the concentrations are much more similar between the neutral and convective cases than for NO_x.

4. Integral street-canyon model including trees

An integral model has been developed to aid understanding of this complex problem. The model detailed below explains the effects that trees have on urban air quality. Extending the standard integral model for pollution in street canyons (Nunez and Oke, 1977; Soulhac et al., 2013) with the effect of trees results in

$$\Lambda W H \frac{\mathrm{d}\langle\varphi\rangle_c}{\mathrm{d}t} = Q_\varphi \Lambda - u_e W \Lambda (\langle\varphi\rangle_c - \varphi_B) - a u_d A_t \Lambda \langle\varphi\rangle_c. \tag{10}$$

Here, $\langle\varphi\rangle_c$ is the canyon-averaged concentration, φ_B is the background concentration, Λ is the canyon length, W is the canyon width, H is the canyon height, Q_φ is the scalar line source, A_t is the area occupied by trees in cross-section and u_e is the exchange velocity. In a steady-state situation, the concentration in the street is given by

$$\langle\varphi\rangle_c = \frac{\varphi_B + \frac{Q_\varphi}{u_e W}}{1 + \frac{u_d}{u_e}\frac{a A_t}{W}}. \tag{11}$$

In order to get an idea of the sensitivity of the equation above to the presence of trees, a Taylor series expansion is performed around $a = 0$, noting that the exchange velocity is affected by the presence of trees and thus $u_e = u_e(a)$:

$$\langle\varphi\rangle_c = \varphi_B + \frac{Q_\varphi}{W u_{e0}}\left[1 - \frac{1}{u_{e0}}\frac{\mathrm{d}u_e}{\mathrm{d}a}a\right] - \left(\varphi_B + \frac{Q_\varphi}{W u_{e0}}\right)\frac{u_d}{u_{e0}}\frac{a A_t}{W} + O(a^2). \tag{12}$$

This equation demonstrates that the deposition on the leaves acts to reduce the concentration, but a reduction in the exchange velocity u_e due to the presence of trees will act to increase the concentration. Denoting the concentration without trees present as $\langle\varphi\rangle_{c0} = \varphi_B + Q_\varphi/(u_e W)$, we can rewrite this equation as

$$\frac{\langle\varphi\rangle_c}{\langle\varphi\rangle_{c0}} = 1 - \frac{Q_\varphi}{W\langle\varphi\rangle_{c0} u_{e0}^2}\frac{\mathrm{d}u_e}{\mathrm{d}a}a - \frac{u_d}{u_{e0}}\frac{a A_t}{W} + O(a^2). \tag{13}$$

The air quality will improve if

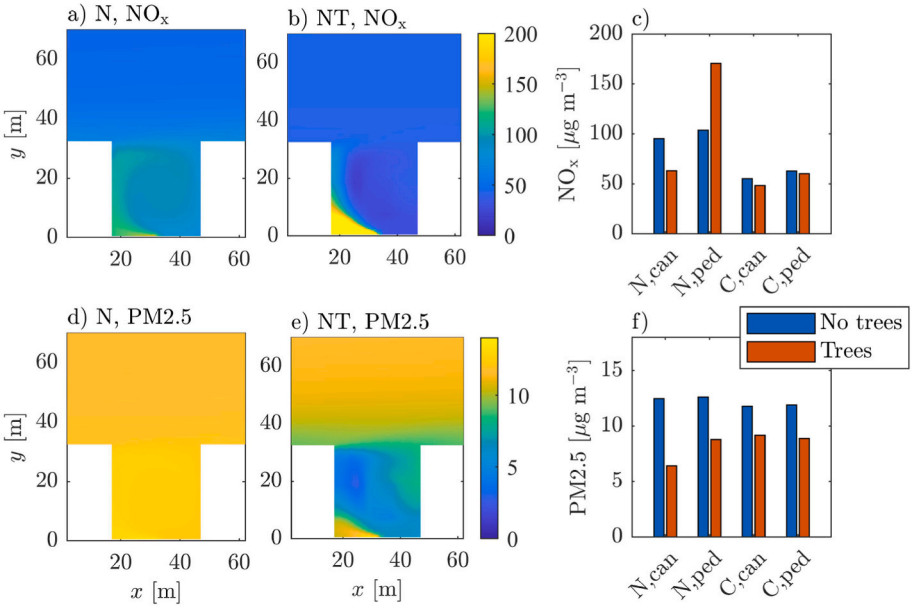

Fig. 8. Time- and spanwise-averaged pollutant concentrations for NO_x and PM2.5 in the eighth canyon from the inlet boundary. NO_x concentration for the neutral case a) without trees (N), b) with trees (NT). c) canyon-averaged and pedestrian-height-averaged NO_x concentration for all four cases. PM2.5 concentration for the neutral case d) without trees (N), e) with trees (NT). f) canyon-averaged and pedestrian-height-averaged PM2.5 concentration for all four cases.

$$-\frac{Q_\varphi}{W\langle\varphi\rangle_{c0}u_{e0}^2}\underbrace{\frac{\mathrm{d}u_e}{\mathrm{d}a}}_{-\delta u_e}a < \frac{u_d}{u_{e0}}\frac{aA_t}{W} \quad \Leftrightarrow \quad \delta u_e < \frac{\langle\varphi\rangle_{c0}}{\langle\varphi\rangle_{c0}-\varphi_B}\frac{aA_t}{W}u_d. \tag{14}$$

In the second step, we defined the (positive) difference in exchange velocity between the no-tree and tree scenarios as $\delta u_e \equiv -a\mathrm{d}u_e/\mathrm{d}a$. This is justified since $\mathrm{d}u_e/\mathrm{d}a$ is constant due to the Taylor series expansion, which implies that $a\mathrm{d}u_e/\mathrm{d}a$ represents the difference in exchange velocity between the no-tree and the tree scenario. The only variables that are not known in the expression above are the concentration in absence of trees $\langle\varphi\rangle_{c0}$ and the change in exchange velocity due to the presence of trees δu_e (how the tree affects the breathability of the street canyon).

Two limiting scenarios can now be identified: 1) the emissions dominate the canyon concentration; and 2) the background concentration dominates the canyon concentration. When emissions dominate, $\langle\varphi\rangle_{c0} \gg \varphi_B$, the criterion for improvement of air quality (14) simplifies to

$$\delta u_e < \frac{aA_t}{W}u_d \tag{15}$$

in which the right-hand side can be calculated *a priori*. This implies that when the pollution is emissions-dominated, trees can both enhance and deteriorate air quality. When the background concentration dominates, we have $\langle\varphi\rangle_{c0} \approx \varphi_B$, (14) becomes

$$\delta u_e < \infty \tag{16}$$

This implies that when the air pollution is background-dominated, trees are guaranteed to improve air quality.

The predictions of this model are largely consistent with the results for NO_x and PM2.5 in the previous section. For the PM2.5 scenario, which is background-concentration-dominated, the air quality improves for both situations considered. For the NO_x scenario, δu_e needs to be smaller than 0.05 m s^{-1} in order to improve the air quality. The quantity δu_e can be calculated from the simulations by taking the difference in exchange velocity u_e between the tree and no-tree case. From Table 2 we infer that for the neutral case, $\delta u_e = 0.03 < 0.05$ m s^{-1} and thus the canyon-averaged air quality is expected to improve. This is consistent with Fig. 8c. For the convective case, $\delta u_e = 0.10 > 0.05$ m s^{-1} and the canyon-averaged concentration is expected to deteriorate. This is not consistent with the tree and no tree convective simulations (C and CT), which show that the canyon-average air quality (slightly) improves due to the presence of the trees. This difference is due to the simplifying assumptions made in the model development.

5. Discussion

The complex interactions between trees and the surrounding urban environment result in situations where local air pollution concentrations can both increase or decrease due to the presence of a tree. Whilst trees actively remove pollutants from the urban atmosphere (deposition effect), they also affect the dispersion of pollutants within and out of street canyons by altering the flow of air (dispersion effect; driven by drag and energy balance changes). A trees' impact on the surrounding air quality is driven by the balance between these processes. In this study, the idealised case of trees in an infinite street canyon was used as a mechanism to better understand how this deposition-dispersion relationship plays out in urban areas.

A key finding is that the effect of a tree on urban air quality varies depending on the prevalence of local emission sources. The street type and pollutant therefore play a big role in determining the effect of the tree. For streets or pollutants where the local concentration is dominated by background levels, the removal of pollutants by the tree canopy via deposition will dominate and the tree will generally act to improve the local air quality. This case is analogous of 1) urban trees that are not located close to significant emission sources (e.g. pedestrianised streets, low traffic streets, and streets where building emissions are at roof not street level) and 2) pollutants that exist relatively more homogeneously in the urban environment (e.g. cases where roadside PM2.5 levels are dominated by transboundary and background levels).

The potential for trees to have an adverse effect on local pollution concentrations increases with increasing prevalence of local emission sources. Scenarios that are conducive of this effect include busy, congested streets, streets with high level of emissions from other sources such as outdoor street vendors or waste burning, and pollutants that are more spatially variable within cities, such as NO_x.

There are two ways in which increased concentrations could occur due to the presence of a tree. Firstly, the tree canopy can inhibit the dispersion or 'mixing' of air pollutants close to the source resulting in local hotspots within the canyon, often at pedestrian level (as illustrated by pedestrian level concentrations for the neutral case in Section 3.4). The second way trees may result in increased concentrations is by affecting the rate at which a pollutant is removed from the street canyon and dispersed into the atmosphere above. The street-atmosphere interaction will be affected by changes to the air flow within the canyon due to the presence of a tree δu_e. Trees can affect the interaction both by imposing drag that affects the canyon vortex and by providing shading and transpiration that affects the local energy balance and sources of buoyancy. This process is strongly influenced by characteristics such as the size and density of the tree canopy and the local meteorological conditions.

The integral street-canyon model developed in Section 4 parameterises the trade off between the deposition and dispersion effect of trees. This model provides a way to estimate the impact of trees on local air quality using five parameters. Fig. 9 summarises the above discussion in two charts by comparing the tree deposition velocity u_d to its propensity to inhibit the removal of a pollutant out of the canyon, characterised by δu_e. Fig. 9a illustrates the limit case where in-canyon emission sources are negligible and the tree can only have a positive effect via deposition. Fig. 9b draws the line between the tree helping or hindering local pollution concentrations. The relevant parameters were estimated for the simulations outlined in Section 2.3 and are shown by the markers. For the situation considered here, the integral model predicts that trees are expected to improve urban air quality under neutral conditions, but worsen it under convective conditions where the tree had a larger effect on the exchange velocity.

The integral street-canyon model with trees therefore provides a simplistic design tool to estimate whether trees will help or hinder urban air quality. However, it is important to note that there are limitations to this idealised case, and that it can be challenging to identify values for u_d and δu_e. Wang et al. (2019) highlight the challenges of determining u_d accurately for different tree types and pollutant species. They also indicate that values of u_d used in the majority of modelling studies have been underestimated, suggesting that the deposition effect of trees will be more significant than what was used above. Determining u_e in absence of trees is an established area of research (Salizzoni et al., 2011). However, the integral street-canyon model with trees requires comparing the value of u_e for a street canyon without trees to that with trees, thereby obtaining δu_e. Studies have explored with and without tree cases in wind tunnel experiments (Gromke and Ruck, 2012; Fellini, 2021), but there are currently no methods available to estimate δu_e *a priori*.

The sensitivity of the relationship illustrated in Fig. 9b needs to be explored further. Different street geometries, flow regimes, meteorological conditions, tree sizes, tree types and pollutant species need to be explored to map out how often trees improve and worsen urban air quality. Control tests (large-eddy simulations and wind tunnel experiments) should be used to test this sensitivity and parameterise δu_e. It is also useful to put the idealised case of trees in an infinite street canyon in the context of other key urban design factors. Street canyons vary in aspect ratios: narrower streets have multiple vortices, which trees will interact with differently and wider streets lead to wake interference and isolated roughness flow regimes where the typical shear layer assumptions for u_e do not hold. Real urban morphologies are complex and finite

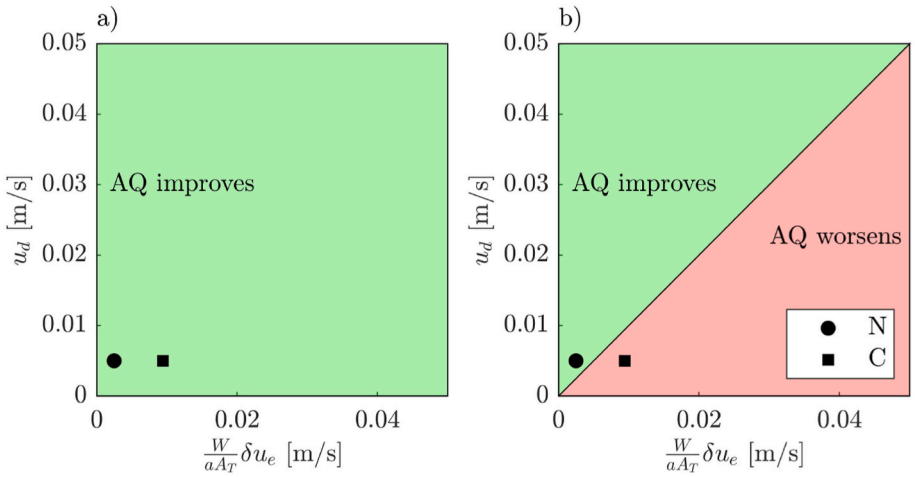

Fig. 9. The effect of trees on canyon-averaged concentration for a) background-concentration-dominated scenarios and b) canyon-emissions-dominated scenarios.

length streets with intersections and variable height buildings have advective fluxes out of the street canyons that also impact u_e.

Many studies have considered the use of green barriers as opposed to trees (Barwise and Kumar, 2020; Diener and Mudu, 2021; Pugh et al., 2012). The positioning and size of barriers within the street minimise the blocking effect on the canyon vortex and their proximity to emission sources are advantageous to the trees considered here. This scenario is different than that considered here. Indeed, in this paper, the trees provide a barrier between the road and the atmosphere. A correctly functioning vegetation barrier will reduce direct exposure, and encourages dilution within the canyon and exchange with the atmosphere before exposure occurs, thereby improving air quality.

6. Conclusion

The tree model presented in Grylls and van Reeuwijk (2021) and an integrated street model, adapted to include trees, were used to study the effect of trees on urban on air quality. The simplified case of trees in an infinite street canyon was used to provide generalised insights on the key mechanisms through which trees can both help and hinder local air quality: deposition and dispersion.

Cases with and without trees and under neutral and convective conditions were first studied using large-eddy simulations (LES). Trees' effects on air quality were systematically studied by simulating background pollution levels independently from the locally-emitted pollutants, and applying weighting factors to study effects on different pollutants species and street types (capitalising on the linearity of the scalar transport). The prevalence of local, in-canyon emissions versus background levels was shown to be a fundamental determinant of the localised impact of a tree. For background-dominated concentration fields, analogous of PM2.5 levels or quiet streets, the presence of a tree resulted in improvements in the local air quality across all scales in these simulations. For the case considered, the canyon-averaged pollutant concentration of effective PM2.5 was reduced by 49% and 22% due to the presence of trees under the neutral and convective conditions respectively. This phenomenon is driven by the deposition effect of trees canopies, which for these more spatially homogeneous pollutant fields dominated over any dispersion effects. For emissions-dominated concentrations fields, these dispersion effects of trees (driven by the drag imposed on the local air flow and the change in buoyancy distribution due to tree shading and transpiration) can counteract the benefits of deposition. These cases are analagous of pollutant species like NO_x on busy roads with significant street-level emissions. The simulation results illustrated that, under these conditions, pollutant hotspots can form close to the sources at pedestrian level as pollutants are dispersed less effectively away from their source. Pedestrian-level concentrations of effective NO_x increased by 64% under neutral conditions, although decreased by 4% under convective conditions where the blocking effect was reduced due to buoyancy impacts on the flow structure. In terms of canyon-averaged concentrations, the deposition effects still dominated over changes in exchange of pollutants out of the canyon and trees acted to improve overall air quality in the case considered in this study.

The intricacies of this deposition-dispersion relationship were interrogated through analysis of the impact of the trees on the flow field and buoyancy distribution within the canyon. For the case considered in this study, trees were shown to significantly affect the flow structure within the canyon (67% average reduction in the wind speed). The sensible heat flux from the tree canopies altered the flow structure for the convective case, particularly in terms of the flow direction around the windward tree canopy. The presence of trees under convective conditions resulted in a cooling of the air. The canyon- and pedestrian-averaged temperatures were reduced by 0.23 and 0.83 K respectively in these simulations. As a result of the strong radiative conditions, the cooling effect was attributed largely to the tree shading effect (the net sensible heat flux from the tree canopy was positive). It was shown that thermal effects of trees are important to consider when studying the impact of trees on urban air quality. The infinite canyon study presents a show-case investigation into urban trees using LES. More extensive studies are required using the tree model to explore the large parameter space and complex system sensitivities.

To further explore these findings, in lieu of additional LES, experimental or field studies, an integral model was developed to capture the idealised canyon-averaged effect of trees on local air quality with minimal parameters. The integral model simplistically captures the effects discussed above by breaking the deposition-disperison relationship into two parameters. It provides an urban design tool through which it is possible to determine cases where local air quality will be either improved or worsened by the presence of a tree.

CRediT authorship contribution statement

Tom Grylls: Conceptualization, Methodology, Software, Formal analysis, Investigation, Writing – original draft, presentation. **Maarten van Reeuwijk:** Conceptualization, Methodology, Supervision, Writing – review & editing.

Declaration of competing interest

The authors declare that they have no known competing financial interests or personal relationships that could have appeared to influence the work reported in this paper.

Data availability

Data will be made available on request.

Acknowledgments

The computational resources for this work were provided by the Imperial College HPC facilities and the UK National Supercomputing Service, ARCHER. The latter computations were supported by the EPSRC-funded UK Turbulence Consortium (grant reference EP/R029326/1). T.G. would like to acknowledge support by the EPSRC Centre for Doctoral Training in Sustainable Civil Engineering (grant reference EP/L016826/1).

List of Symbols

Symbols

α	Extinction coefficient (−)
δu_e	Difference in exchange velocity between no-tree and tree case (m s^{-1})
Λ	Canyon length (m)
φ_θ	Temperature flux (K m s^{-1})
φ_{q_v}	Water vapour specific humidity flux (kg kg^{-1} m s^{-1})
ρ	Density of air (kg m^{-3})
τ	Eddy turnover time (s)
θ	Potential temperature (K)
φ	Pollution concentration (- or μg m^{-3})
A	Area (m^2)
a	Leaf-area density (m^2 m^{-3})
c_1, c_2	Weightings for superposition of scalar fields (−)
C_d	Drag coefficient (−)
c_p	Heat capacity (J K^{-1})
d	Leaf area index (−)
H	Canyon height (m)
h	Boundary layer/domain height (m)
l	Leaf size (m)
$L(L_{\min})$	(Minimum) Obukhov length (m)
L_v	Latent heat of vapourisation (J kg^{-1})
Q^*	Net radiation (W m^{-2})
Q_φ	Pollution line source (m^2 s^{-1} or μg m^{-1} s^{-1})
Q_E	Latent heat flux (W m^{-2})
Q_H	Sensible heat flux (W m^{-2})
q_v	Water vapour specific humidity (kg kg^{-1})
r_s	Stomatal resistance (s m^{-1})
S, R	Volumetric source/sink terms (−)
T	Temperature (K)
u^*	Friction velocity (m s^{-1})
u_d	Deposition velocity (m s^{-1})
u_e	Exchange velocity (m s^{-1})
u_i	Wind velocity (m s^{-1})
V	Volume (m^3)
W	Canyon width (m)
w^*	Deordorff scale (m s^{-1})

Abbreviations

NTC	Net tree cooling (−)
TCR	Tree cooling ratio (−)

Subscripts

$\cdot_a$	Denoting values attributed to the atmosphere
$\cdot_b$	Denoting values attributed to background scalar fields
$\cdot_c$	Denoting net values attributed to canyon averages
$\cdot_e$	Denoting values attributed to emitted scalar fields
$\cdot_l$	Denoting values attributed to leaves
$\cdot_p$	Denoting averaging across a canyon at pedestrian height
$\cdot_s$	Denoting values attributed to shaded horizontal surfaces
$\cdot_t$	Denoting net values attributed to tree canopies
$\cdot_u$	Denoting values attributed to unshaded horizontal surfaces

References

Abhijith, K., Kumar, P., Gallagher, J., McNabola, A., Baldauf, R., Pilla, F., Broderick, B., Di Sabatino, S., Pulvirenti, B., 2017. Air pollution abatement performances of green infrastructure in open road and built-up street canyon environments–a review. Atmos. Environ. 162, 71–86.

Aboelata, A., 2020. Vegetation in different street orientations of aspect ratio (h/w 1: 1) to mitigate uhi and reduce buildings' energy in arid climate. Build. Environ. 172, 106712.

Akbari, H., Rosenfeld, A.H., Taha, H., 1990. Summer heat islands, urban trees, and white surfaces. In: Proceedings of the 1990 ASHRAE Winter Conference, p. 1381.

Akbari, H., Pomerantz, M., Taha, H., 2001. Cool surfaces and shade trees to reduce energy use and improve air quality in urban areas. Sol. Energy 70, 295–310.

Allegrini, J., Dorer, V., Carmeliet, J., 2014. Buoyant flows in street canyons: validation of cfd simulations with wind tunnel measurements. Build. Environ. 72, 63–74.

Barlow, J.F., Harman, I.N., Belcher, S.E., 2004. Scalar fluxes from urban street canyons. part i: laboratory simulation. Boundary-Layer Meteorol. 113, 369–385.

Barwise, Y., Kumar, P., 2020. Designing vegetation barriers for urban air pollution abatement: a practical review for appropriate plant species selection. Npj Climate and Atmospheric Science 3, 1–19.

Batchvarova, E., Gryning, S.E., 1991. Applied model for the growth of the daytime mixed layer. Boundary-Layer Meteorol. 56, 261–274.

Bowler, D.E., Buyung-Ali, L., Knight, T.M., Pullin, A.S., 2010. Urban greening to cool towns and cities: a systematic review of the empirical evidence. Landsc. Urban Plann. 97, 147–155.

Buccolieri, R., Salim, S.M., Leo, L.S., Di Sabatino, S., Chan, A., Ielpo, P., de Gennaro, G., Gromke, C., 2011. Analysis of local scale tree–atmosphere interaction on pollutant concentration in idealized street canyons and application to a real urban junction. Atmos. Environ. 45, 1702–1713.

Buccolieri, R., Santiago, J.L., Rivas, E., Sanchez, B., 2018. Review on urban tree modelling in cfd simulations: aerodynamic, deposition and thermal effects. Urban For. Urban Green. 31, 212–220.

Businger, J., 1973. A note on free convection. Boundary-Layer Meteorol. 4, 323–326.

CERC, 2001. ADMS-urban User Manual. Technical Report. CERC.

King's College London, 2019. London average air quality levels. URL: https://data.london.gov.uk/dataset/london-average-air-quality-levels. (Accessed 3 January 2022).

Diener, A., Mudu, P., 2021. How can vegetation protect us from air pollution? a critical review on green spaces' mitigation abilities for air-borne particles from a public health perspective-with implications for urban planning. Sci. Total Environ. 796, 148605.

Fellini, S., 2021. Modelling Pollutant Dispersion at the City and Street Scales. École Centrale de Lyon. Ph.D. thesis.

Fu, X., Xiang, S., Liu, Y., Liu, J., Yu, J., Mauzerall, D.L., Tao, S., 2020. High-resolution simulation of local traffic-related NOx dispersion and distribution in a complex urban terrain. Environ. Pollut. 263, 114390.

Grimmond, C.S.B., Oke, T.R., 1991. An evapotranspiration-interception model for urban areas. Water Resour. Res. 27, 1739–1755.

Gromke, C., Ruck, B., 2012. Pollutant concentrations in street canyons of different aspect ratio with avenues of trees for various wind directions. Boundary-Layer Meteorol. 144, 41–64.

Gromke, C., Blocken, B., Janssen, W., Merema, B., van Hooff, T., Timmermans, H., 2015. Cfd analysis of transpirational cooling by vegetation: case study for specific meteorological conditions during a heat wave in arnhem, Netherlands. Build. Environ. 83, 11–26.

Grylls, T., 2019. Simulating Air Pollution in the Urban Microclimate. Ph.D. thesis. Imperial College London.

Grylls, T., van Reeuwijk, M., 2021. Tree model with drag, transpiration, shading and deposition: identification of cooling regimes and large-eddy simulation. Agric. For. Meteorol. 298, 108288.

Grylls, T., Le Cornec, C.M., Salizzoni, P., Soulhac, L., Stettler, M.E.J., van Reeuwijk, M., 2019. Evaluation of an operational air quality model using large-eddy simulation. Atmos. Environ. X 3, 100041.

Grylls, T., Ivo, S., van Reeuwijk, M., 2020. Steady-state large-eddy simulations of convective and stable urban boundary layers. Boundary-Layer Meteorol. 175, 309–341.

Grylls, T., Suter, I., Sützl, B., Owens, S., Meyer, D., van Reeuwijk, M., 2021. udales: large-eddy-simulation software for urban flow, dispersion, and microclimate modelling. J. Open Source Software 6, 3055.

Heus, T., Vilà-Guerau de Arellano, J., De Roode, S., Pino González, D., Van Heerwaarden, C.C., Jonker, H.J.J., Siebesma, P., Axelsen, S., Van den Dries, K., Geoffroy, O., et al., 2010. Formulation of the Dutch atmospheric large-eddy simulation (dales) and overview of its applications. Geosci. Model Dev. (GMD) 3, 415–444.

Hundsdorfer, W., Koren, B., Verwer, J.G., et al., 1995. A positive finite-difference advection scheme. J. Comput. Phys. 117, 35–46.

Janhäll, S., 2015. Review on urban vegetation and particle air pollution–deposition and dispersion. Atmos. Environ. 105, 130–137.

Jeanjean, A.P., Buccolieri, R., Eddy, J., Monks, P.S., Leigh, R.J., 2017. Air quality affected by trees in real street canyons: the case of marylebone neighbourhood in central london. Urban For. Urban Green. 22, 41–53.

Jones, H.G., 2013. Plants and Microclimate: a Quantitative Approach to Environmental Plant Physiology. Cambridge university press.

Kim, J.J., Baik, J.J., 2001. Urban street-canyon flows with bottom heating. Atmos. Environ. 35, 3395–3404.

Li, Q., Wang, Z.H., 2018. Large-eddy simulation of the impact of urban trees on momentum and heat fluxes. Agric. For. Meteorol. 255, 44–56.

Li, X.X., Britter, R.E., Koh, T.Y., Norford, L.K., Liu, C.H., Entekhabi, D., Leung, D.Y., 2010. Large-eddy simulation of flow and pollutant transport in urban street canyons with ground heating. Boundary-Layer Meteorol. 137, 187–204.

Li, X.X., Britter, R.E., Norford, L.K., Koh, T.Y., Entekhabi, D., 2012. Flow and pollutant transport in urban street canyons of different aspect ratios with ground heating: large-eddy simulation. Boundary-Layer Meteorol. 142, 289–304.

Manickathan, L., Defraeye, T., Allegrini, J., Derome, D., Carmeliet, J., 2018. Parametric study of the influence of environmental factors and tree properties on the transpirative cooling effect of trees. Agric. For. Meteorol. 248, 259–274.

Morakinyo, T.E., Kong, L., Lau, K.K.L., Yuan, C., Ng, E., 2017. A study on the impact of shadow-cast and tree species on in-canyon and neighborhood's thermal comfort. Build. Environ. 115, 1–17.

Nowak, D., Heisler, G., 2010. Air quality effects of urban trees and parks. In: Research Series Monograph, vol. 44. National Recreation and Parks Association Research Series Monograph, Ashburn, VA, pp. 1–44.

Nunez, M., Oke, T.R., 1977. The energy balance of an urban canyon. J. Appl. Meteorol. Climatol. 16, 11–19.

Oke, T.R., Mills, G., Christen, A., Voogt, J.A., 2017. Urban Climates. Cambridge University Press.

Pugh, T.A., MacKenzie, A.R., Whyatt, J.D., Hewitt, C.N., 2012. Effectiveness of green infrastructure for improvement of air quality in urban street canyons. Environ. Sci. Technol. 46, 7692–7699.

Sæbø, A., Popek, R., Nawrot, B., Hanslin, H.M., Gawronska, H., Gawronski, S.W., 2012. Plant species differences in particulate matter accumulation on leaf surfaces. Sci. Total Environ. 427, 347–354.

Salim, S.M., Buccolieri, R., Chan, A., Di Sabatino, S., Cheah, S.C., 2011. Large eddy simulation of the aerodynamic effects of trees on pollutant concentrations in street canyons. Proc. Environ. Sci. 4, 17–24.

Salim, M.H., Schlünzen, K.H., Grawe, D., 2015. Including trees in the numerical simulations of the wind flow in urban areas: should we care? J. Wind Eng. Ind. Aerod. 144, 84–95.

Salizzoni, P., Soulhac, L., Mejean, P., 2009. Street canyon ventilation and atmospheric turbulence. Atmos. Environ. 43, 5056–5067.

Salizzoni, P., Marro, M., Soulhac, L., Grosjean, N., Perkins, R.J., 2011. Turbulent transfer between street canyons and the overlying atmospheric boundary layer. Boundary-Layer Meteorol. 141, 393–414.

Santiago, J.L., Martilli, A., Martin, F., 2017. On dry deposition modelling of atmospheric pollutants on vegetation at the microscale: application to the impact of street vegetation on air quality. Boundary-Layer Meteorol. 162, 451–474.

Soulhac, L., Salizzoni, P., Cierco, F.X., Perkins, R., 2011. The model SIRANE for atmospheric urban pollutant dispersion; PART I, Presentation of the model. Atmos. Environ. 45, 7379–7395.

Soulhac, L., Salizzoni, P., Mejean, P., Perkins, R.J., 2013. Parametric laws to model urban pollutant dispersion with a street network approach. Atmos. Environ. 67, 229–241.

Stull, R.B., 2012. An Introduction to Boundary Layer Meteorology, vol. 13. Springer Science & Business Media.

Suter, I., 2018. Simulating the Impact of Blue-Green Infrastructure on the Microclimate of Urban Areas. Ph.D. thesis. Imperial College London.

Suter, I., Grylls, T., Sützl, B., van Reeuwijk, M., 2020. Udales: a Large-Eddy-Simulation Model for Urban Environments. Geoscientific Model Development [in preparation].

Suter, I., Grylls, T., Sützl, B., van Reeuwijk, M., 2021. Udales 1.0. 0: a large-eddy-simulation model for urban environments. Geosci. Model Dev. Discuss. (GMDD) 1–40.

Sützl, B.S., Rooney, G.G., van Reeuwijk, M., 2021. Drag distribution in idealized heterogeneous urban environments. Boundary-Layer Meteorol. 178, 225–248.

Tomas, J.M., Pourquie, M.J.B.M., Jonker, H.J.J., 2016. Stable stratification effects on flow and pollutant dispersion in boundary layers entering a generic urban environment. Boundary-Layer Meteorol. 159, 221–239.

Wang, H., Maher, B.A., Ahmed, I.A., Davison, B., 2019. Efficient removal of ultrafine particles from diesel exhaust by selected tree species: implications for roadside planting for improving the quality of urban air. Environ. Sci. Technol. 53, 6906–6916.

Zhou, S., Lin, R., 2019. Spatial-temporal heterogeneity of air pollution: the relationship between built environment and on-road pm2. 5 at micro scale. Transport. Res. Transport Environ. 76, 305–322.